Omnidirectional Dual-Reflector Antennas for High Directivity over Wideband in Millimeter Waves

Rafael A. Penchel[1], Sandro R. Zang[2], José R. Bergmann[3], Fernando J. S. Moreira[4]
[1]Department of Electrical Engineering, UTFPR, Cornélio Procópio, Brazil, penchel@uftpr.edu.br
[2] Department of Mechatronics and Telecommunication Engineering, UFSJ, Ouro Branco, Brazil, szang@ufsj.edu.br
[3] Center for Telecommunication Studies, PUC-Rio, Rio de Janeiro, Brazil, bergmann@cetuc.puc-rio.br
[4] Department of Electronics Engineering, UFMG, Belo Horizonte, Brazil, fernandomoreira@ufmg.br

***Abstract* — This work presents a study of the electromagnetic performance of classical and shaped omnidirectional dual-reflector antennas in millimeter waves. An algorithms based on the concatenation of conic sections has been used to synthesize sub- and main-reflectors in order to provide a uniform phase and amplitude aperture distributions. The frequency analysis is focused on antenna radiation patterns across a 20% bandwidth, in order to establish band limits for omnidirectional dual-reflector antennas. The rigorous electromagnetic analysis was accomplished by a hybrid technique based on Mode Matching and Method of Moments.**

***Index Terms* — Reflector antennas, omnidirectional dual-reflector antennas, millimeter wave antennas**

I. INTRODUCTION

The tremendous growth of data rates required by new communication services has forced the development of systems operating in higher frequencies, like millimeter wave band, where the spectrum is less congested. At these frequencies, there are several differences between communication systems, notably high propagation loss and large sensitivity to blockage [1]. Recent researches have suggested millimeter wave frequencies for the operation of the next generation of broadband mobile communication [2]. Currently, there is a huge effort of researchers to characterize the frequency bands at 28 GHz, 38 GHz, 60 GHz and 73 GHz [3], [4]. At these frequencies, highly-efficient shaped omnidirectional reflector antennas can be suited to provide broadband communication.

Much has been done concerning GO – Geometrical Optics – synthesis of omnidirectional dual-reflector antennas [5]–[12]. In [5]–[7] techniques were explored for shaping axis-symmetric dual-reflector antennas designed to offer omnidirectional coverage with an arbitrary radiation pattern in the vertical elevation plane. To design highly directive antennas, another formulation was derived to shape sub- and main-reflectors of omnidirectional dual-reflector antennas with a prescribed equiphase aperture field distribution [8]. In both cases, GO principles were used to formulate the problem in terms of ordinary differential equations. In [9]–[12] a shaping technique based on the combination of local conic sections was presented, which proved to be simpler and more efficient for many circularly symmetric dual-reflector configurations.

In GO designs, it is highly desired stability of the feed-phase center position, as well a steady radiation pattern over the operating bandwidth. However, obtaining this type of behavior in a very large frequency band is extremely difficult. Consequently, the radiation pattern of the reflector tends to move away from the desired extent with frequency. In [13] it was shown that, across a 10% bandwidth, the radiation patterns of classical omnidirectional dual-reflector configurations have gains with a maximum variation of 0.7 dB. The shaped antennas designed to provide a cosecant-squared pattern in the elevation plane present more incisive differences and the specifications were not sustained across the bandwidth.

The present study investigates the electromagnetic performance of omnidirectional dual-reflector antennas designed to operate at 28 GHz across a 20% bandwidth. The omnidirectional axis-displaced Cassegrain (OADC) and omnidirectional axis-displaced ellipse (OADE) configurations were choosen in order to obtain more compact dual-reflector arrangements [14], [15]. Classical configurations and shaped reflector arrangements with uniform phase and amplitude aperture distributions in the elevation plane are considered. This investigation pretends to determine the effects of the GO shaping in the wide operation bandwidth of these antennas. To estimate the electromagnetic performance, a rigorous analysis is employed, combining the Mode Matching Technique (MMT) to account for the fields inside the coaxial horn and the Method of Moments (MoM) to simulate the electromagnetic radiation from both reflector surfaces [16].

II. SYNTHESIS AND ANALYSIS TECHNIQUES

In order to characterize the electromagnetic behavior of the omnidirectional dual-reflector antennas, two different reflector arrangements were chosen: classical antennas – that is, circularly symmetric sub- and main-reflector surfaces are generated by conic sections –, and both sub- and main reflector shaped to provide high directivity with uniform phase and amplitude field at the aperture.

The design procedure of classical omnidirectional dual-reflector antennas is extensively discussed in [14] and [15]. For ADC configurations the subreflector is generated by a hyperbola while for ADE configurations the generatrix is an ellipse. In both cases the main-reflector is generated by a

parabola. In this work, it was adopted the formulation presented in [14] in order to control the antenna main-beam direction in the elevation plane, which matches the direction of the generating parabola axis.

The shaping technique adopted in the present work uses a generalization of the formulation presented in [12] to attain an arbitrary main-beam direction in the elevation plane. The subreflector is generated by a combination of local conic sections S_n, sequentially concatenated to each other. Each S_n has a (common) focus at the origin (O) and the other at a caustic region (P_n), as illustrated in Fig. 1 for an ADE configuration. The feed horn has a circularly symmetric radiation pattern $G_F(\theta_F)$, where θ_F is the angle between the feed-ray and the z-axis and its feed phase-center is at O. The main-reflector is formed by a set of parabolic sections M_n with a common axial tilt angle γ in elevation plane. From a GO perspective, the rays emanating from the point source O are reflected by S_n toward P_n. After a second reflection at M_n, the rays arrive at the conical aperture parallel to each other, which provides a uniform aperture phase distribution with a prescribed circularly symmetric power density $G_A(x')$, where x' is the aperture coordinate in the auxiliary coordinate system x', z' (see Fig. 1).

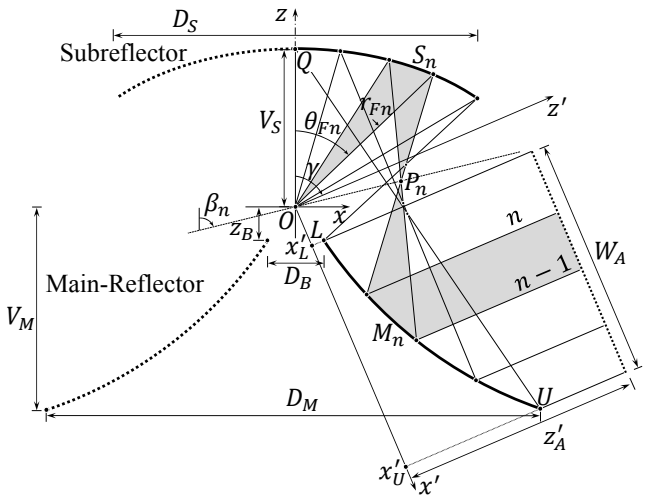

Fig. 1. Basic geometric parameters of a shaped OADE antenna.

In order to estimate the electromagnetic performance of the antenna, a rigorous analysis presented in [16] is employed. The hybrid method combines the Mode Matching Technique (MMT) to treat the fields inside of the coaxial TEM horn, which is represented as series of stepped coaxial waveguide sections, and the Method of Moments (MoM) to solve a combination of electric and magnetic field integral equations to calculate the exterior equivalent surface currents and, consequently, the amplitudes of the modes reflected back into the horn. Figure 2 shows the coaxial horn's far-field radiation patterns from 25 GHz to 31 GHz. Looking at Fig. 2, it is clear one of the most challenging problems to design a reflector antenna system with a large operating bandwidth. The wide variation of the feed radiation pattern with frequency, especially for $\theta_F > 40°$, provides, as a consequence, fluctuations in antenna directivity.

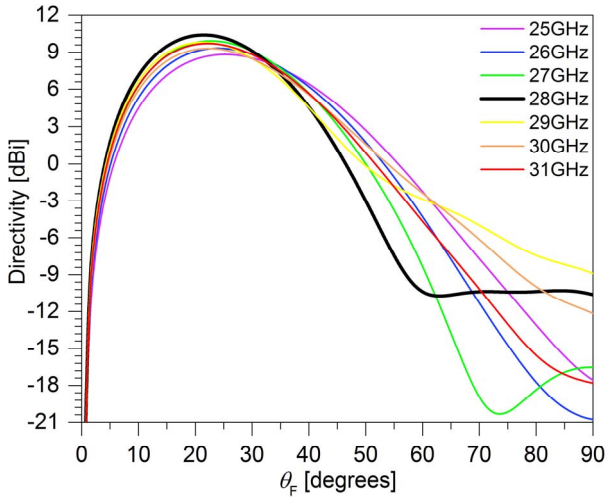

Fig. 2. Coaxial Horn radiation patterns

III. Design Analysis

In this section, several study cases will be presented considering classical and shaped reflector antennas. In the GO synthesis process of shaped configurations, the feed is assumed to be a TEM coaxial horn with a radiation pattern in the far-field region given by [7]:

$$G(\theta_F) = G_0 \left[\frac{J_0(kr_i \sin\theta_F) - J_0(kr_e \sin\theta_F)}{\sin\theta_F} \right]^2 \qquad (1)$$

where G_0 is a normalization factor, $k = 2\pi/\lambda$ is the wave number, $r_i = 0.3\lambda$ and $r_e = 1.17\lambda$ are de internal and external radii of the coaxial aperture, with λ being the wavelength at the central frequency $f = 28$ GHz. The reflector aperture power density distribution $G_A(x')$ is constant in order to obtain highly directive antennas.

A. Classical Omnidirectional Dual-Reflector Antennas

Initially, two classical axis-displaced omnidirectional configurations – an ADE (Case A.I) and an ADC (Case A.II) – were studied. Both antennas were designed to have maximum main-beam direction at $\theta = \gamma = 102°$, main-reflector aperture width $W_A = 12\lambda$, main-reflector diameter $D_M = 26\lambda$, central opening diameter $D_B = 2.4\lambda$, focus O at the plane of the main-reflector central opening ($z_B = 0$), $V_S = 14.0\lambda$ and $V_S = 15.0\lambda$ for the ADE and ADC configurations, respectively. These initial parameters were used together with the formulation presented in [15] to obtain the main and sub-reflector generatrices. For Case A.I the subreflector is generated by an ellipse with an eccentricity equal to $\varepsilon = 0.221419$, an inter-focal distance $2c = 5.794\lambda$, and an axis with tilt angle $\beta = 59.83°$ with respect to the z-axis. As a consequence, the projected diameter of the subreflector is $D_S = 26.229\lambda$ and the subreflector edge angle is $\theta_E = 55.23°$, as shown in Fig. 3. For Case A.II the subreflector is generated by a hyperbola with $\varepsilon = 0.695208$, $2c = 68.295\lambda$ and $\beta = 174.42°$. The projected diameter of the subreflector is $D_S = 32.053\lambda$ and the subreflector edge angle is $\theta_E = 56.69°$, as illustrated in Fig. 4.

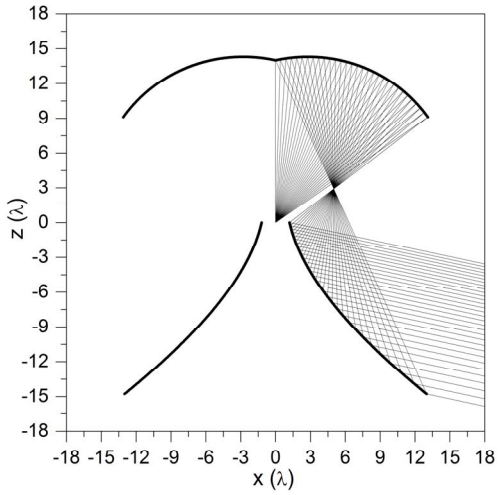

Fig. 3. Generatrices and rays of the classical OADE antenna

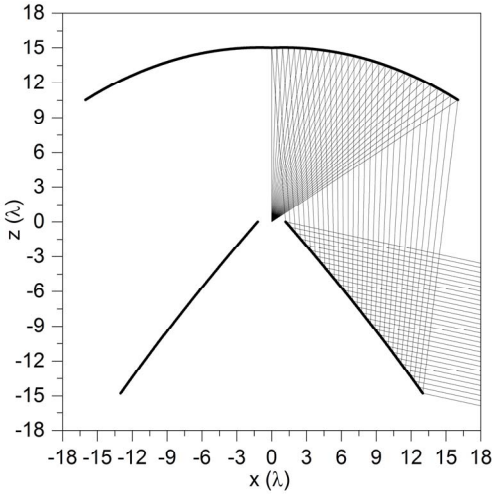

Fig. 4. Generatrices and rays of the classical OADC antenna

TABLE I – GEOMETRIC PARAMETERS OF THE DESIGNED ANTENNAS

	CLASSICAL ANTENNAS		SHAPED ANTENAS	
PARAM.	**CASE A.I**	**CASE A.II**	**CASE B.I**	**CASE B.II**
W_A	12.00λ	12.00λ	12.00λ	12.00λ
D_M	26.00λ	26.00λ	26.00λ	25.55λ
V_M	14.78λ	14.78λ	14.78λ	14.73λ
D_S	26.23λ	32.05λ	27.10λ	31.84λ
V_S	14.00λ	15.00λ	14.00λ	15.00λ
D_B	2.40λ	2.40λ	3.665λ	2.40λ
z_B	0.00λ	0.00λ	-0.1345λ	0.00λ

In order to investigate the bandwidth behaviour of the radiation pattern, the classical omnidirectional ADC and ADE were analysed across a 20% bandwidth – from 25 to 31GHz – by the hybrid technique described in Section II. The corresponding MoM radiation patterns are illustrated in Figs. 5 and 6, for ADE and ADC configurations, respectively. As expected, for both cases the main-beam is directed toward $\theta \approx \gamma = 102°$.

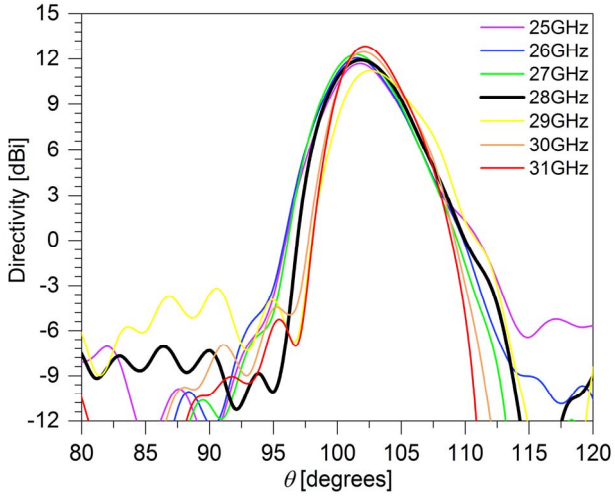

Fig. 5. MoM radiation pattern of classical OADE antenna

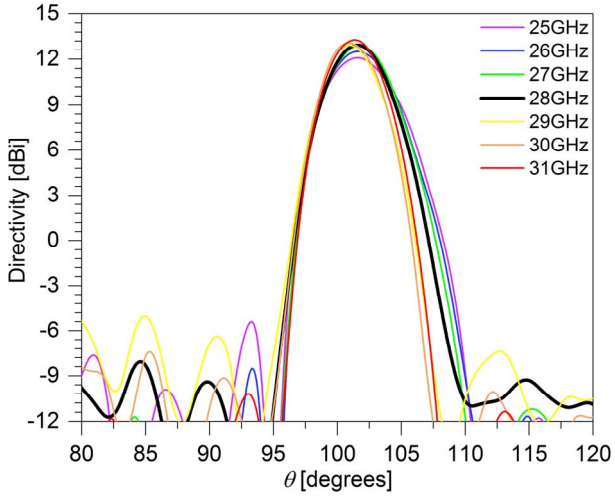

Fig. 6. MoM radiation pattern of classical OADC antenna

TABLE II – DIRECTIVITY OF CLASSICAL ANTENNAS

	CLASSICAL OADE			CLASSICAL OADC		
FREQ. / θ	**101°**	**102°**	**103°**	**101°**	**102°**	**103°**
25GHz	11.58	**11.80**	11.19	12.08	**12.14**	11.50
26GHz	12.10	**12.11**	11.33	12.50	**12.54**	11.93
27GHz	**12.35**	12.30	11.59	12.79	**12.96**	12.37
28GHz	11.82	**12.03**	11.61	12.94	**12.99**	12.13
29GHz	10.33	11.24	**11.26**	**13.12**	12.44	10.86
30GHz	12.13	**12.63**	12.23	**13.20**	12.66	11.27
31GHz	12.30	**12.99**	12.66	**13.35**	13.25	11.92

From the ADE radiation patterns depicted in Fig. 5 one observes that, at 28 GHz, the maximum directivity of 12.03 dBi occurs at $\theta = 102°$. Table II shows the directivity of the radiation patterns as a function of frequency. In bold, the maximum directivity is highlighted. It is observed that, for most of the band, the higher directivities occur at $\theta \approx 102°$ with variations up to 0.96 dB with respect to the central frequency.

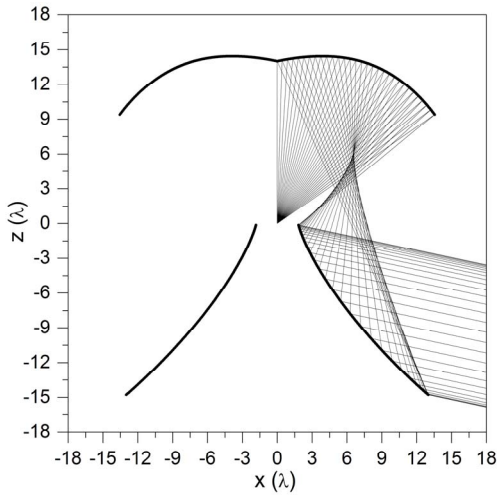

Fig. 7. Generatrices and rays of shaped OADE antenna

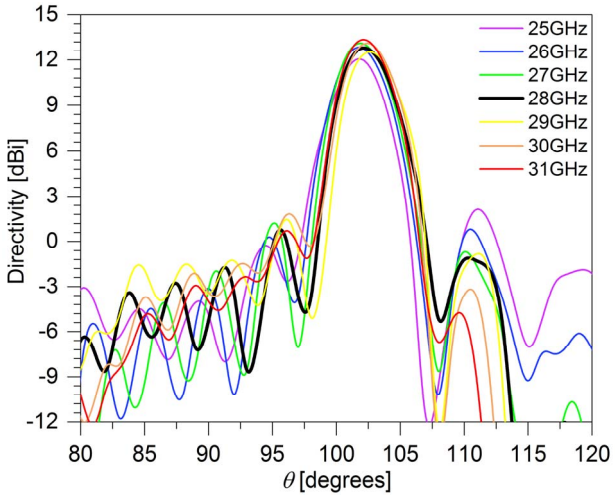

Fig. 9. MoM radiation pattern of shaped OADE antenna

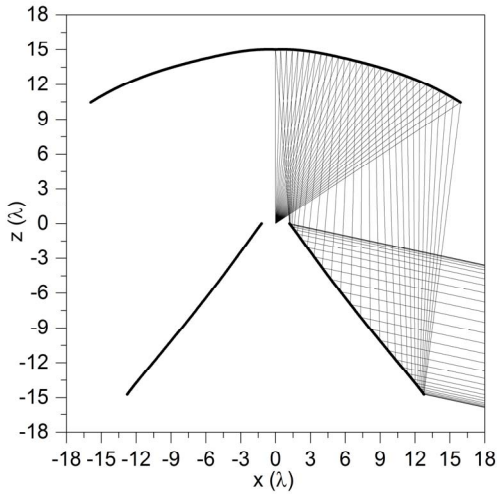

Fig. 8. Generatrices and rays of shaped OADC antenna

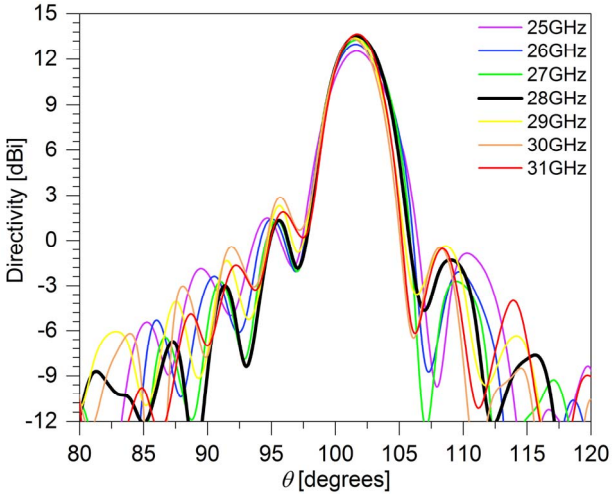

Fig. 10. MoM radiation pattern of shaped OADC antenna

The ADC radiation patterns are depicted in Fig. 6, and it can be observed a directivity of 12.99 dBi at $\theta = 102°$ for the central frequency. From Table I, one observes that the variation in directivity across the 20% bandwidth is about of 0.85 dB. In a visual examination of Figs. 5 and 6, it appears that in the ADE case the variations in the radiation pattern are more significant than in the ADC. This can be imputed to the inversion of the feed illumination toward the main-reflector, a characteristic of ADE configurations. The differences observed in the antenna directivity, for both cases, are mostly due to the variation of the feed-phase center position and the variation of the horn's radiation pattern with frequency, as illustrated in Fig. 2.

B. Shaped Omnidirectional Dual-Reflector Antennas

Using the GO shaping technique described in Section II, an ADE configuration (Case B.I) was designed with uniform amplitude ($G_A = \text{cte.}$) and phase distributions at the tilted conical aperture of the main reflector in order to obtain a highly directive antenna. The feed is assumed to be the same of de Cases A.I and A.II. The design departs from the classical configurations of Case A.I. As a consequence, $D_S = 27.10\lambda$, $D_B = 3.665\lambda$ and $z_B = -0.1345\lambda$, The shaped gerenarticies and ray tracing are shown in Fig. 7. The corresponding ADC configuration (Case B.II) was also designed with uniform amplitude distribution departing from the parameters of the classical antenna of Case A.II. As a result, $D_S = 31.84\lambda$, $D_M = 25.55\lambda$ and $V_M = 14.73\lambda$, as illustrated Fig. 8. For both cases, the other geometrical parameters remain the same of their respective classical configuration (see Table I). Looking to the ray tracing throughout classical (see Figs. 3 and 4) and shaped (see Figs. 7 and 8) configurations, it is possible to observe a higher number of rays in the shaped main reflector edge in order to compensate the lower illumination of the subreflector edge.

The reflector's far-field radiation patterns simulated by the full-wave analysis across a 20% bandwidth are present in Figs. 9 and 10. As expected, the shaped configurations are more directive than the classical ones. The ADE radiation patterns depicted in Fig. 9 show a directivity of 13.00 dBi at $\theta = 102°$ for the central frequency, while the corresponding classical configuration has 12.03 dBi. It should be noted that, for the

entire bandwidth, the shaped antenna is more directive and the radiation patterns are more stable around the main-beam direction. From Table III, one observes variations in the directivity up to 0.70 dB with respect to the central frequency. In bold, the maximum directivity is highlighted.

TABLE III – DIRECTIVITY OF SHAPED ANTENNAS

	SHAPED OADE			SHAPED OADC		
FREQ. / θ	**101°**	**102°**	**103°**	**101°**	**102°**	**103°**
25GHz	11.82	**12.30**	11.16	12.48	**12.66**	11.67
26GHz	12.67	**13.02**	12.02	12.99	**13.05**	12.03
27GHz	12.84	**13.30**	12.54	13.22	**13.37**	12.53
28GHz	12.15	**13.00**	12.54	13.44	**13.64**	12.71
29GHz	10.96	12.50	**12.66**	13.43	**13.49**	12.07
30GHz	11.96	**13.21**	13.10	**13.49**	13.30	11.62
31GHz	12.71	**13.56**	13.04	13.50	**13.87**	12.55

The ADC radiation patterns are presented in Fig. 10. The results confirm the same expectation that the shaped configuration is more divertive than its classical counterpart. It can be observed a directivity of 13.64 dBi at $\theta = 102°$ at the central frequency, 0.65 dB higher than that of the classical antenna. In Fig. 10 the radiation patterns appear to be even more stable than those of Fig. 9. The major variation in directivity was 0.98dB (see Table III) with respect to the central frequency.

IV. CONCLUSIONS

This work discussed the electromagnetic performance of classical and shaped omnidirectional dual-reflector antennas suited to operate in millimetre wave frequencies. First, two classical configurations, an ADE and an ADC, were designed to attain a main-beam direction at $\theta = 102°$ with respect to the symmetry axis. The hybrid technique MoM/MMT was used to analyse the antenna radiation pattern across a 20% bandwidth. It was verified that the antenna's directivities were sustained across the 20% bandwidth with a maximum variation of 0.96 dB (ADE) and 0.85 dB (ADC) with respect to the central frequency.

Shaped omnidirectional dual-reflector antennas were also investigated. An algorithm based on the concatenation of conic sections was used to shape the sub- and main-reflectors in order to provide a uniform phase and amplitude aperture distribution. It was observed that the shaped antennas are more directive than the classical ones and that the radiation patterns are more stable around the main-beam direction. The directivity across the 20% bandwidth presents variations up to 0.70 dB (ADE) and 0.98 dB (ADC) with respect to the central frequency.

ACKNOWLEDGMENT

This work was partially supported by FINEP/FUNTEL Grant No. 01.14.0231.00, under the Radio Communications Reference Center – CRR. Authors also thank the financial support from CNPq and CAPES-PROCAD.

REFERENCES

[1] T. S. Rappaport, R. W. Heath, Jr., R. C. Daniels, and J. N. Murdock, Millimeter Wave Wireless Communications. Englewood Cliffs, NJ, USA: Prentice Hall, 2015.

[2] Z. Pi and F. Khan, "An introduction to millimeter-wave mobile broadband systems," *IEEE Communications Magazine*, vol. 49, pp. 101–107, Jun. 2011.

[3] T. Rappaport, S. Sun, R. Mayzus, H. Zhao, Y. Azar, K. Wang, G. Wong, J. Schulz, M. Samimi, and F. Gutierrez, "Millimeter wave mobile communications for 5G cellular: It will work!," *IEEE Access*, vol. 1, pp. 335–349, May 2013.

[4] T. S. Rappaport, G. R. MacCartney, M. K. Samimi and S. Sun, "Wideband Millimeter-Wave Propagation Measurements and Channel Models for Future Wireless Communication System Design," in *IEEE Trans. on Communications*, vol. 63, no. 9, pp. 3029-3056, Sept. 2015.

[5] A. P. Norris and W. D. Waddoup, "A millimetric wave omnidirectional antenna with prescribed elevation shaping," in Proc. ICAP–4th Int. Conf. Antennas and Propagation, 1985, pp. 141–145.

[6] A. G. Pino, A. M. A. Acuña, and J. O. R. Lopez, "An omnidirectional dual-shaped reflector antenna," Microw. Opt. Tech. Lett., vol. 27, no. 5, pp. 371–374, Dec. 5, 2000.

[7] J. R. Bergmann and F. J. S. Moreira, "Omnidirectional ADE antenna with GO shaped main reflector for arbitrary far-field pattern in the elevation plane," IET Microwaves, Antennas & Propagation, vol. 3, no. 5, pp. 1028–1035, Oct. 2009.

[8] F. Moreira, A. Prata Jr., and J. R. Bergmann, "GO Shaping of Omnidirectional Dual-Reflector Antennas for a Prescribed Equi-Phase Aperture Field Distribution," *IEEE Transactions on Antennas and Propagation*, vol. 55, no. 1, pp. 99–106, Jan. 2007.

[9] Y. Kim and T.-H. Lee, "Shaped circularly symmetric dual reflector antennas by combining local conventional dual reflector systems," IEEE Trans. Antennas Propagat., vol. 57, no. 1, pp. 47–56, Jan. 2009.

[10] F. Moreira and J. Bergmann, "Shaping axis-symmetric dual-reflector antennas by combining conic sections," *IEEE Trans. Antennas Propagation*, vol. 59, pp. 1042–1046, Mar. 2011.

[11] F. Moreira and J. Bergmann, "Omnidirectional Dual-Reflector Shaping by Concatenating Conic Sections", 4th European Conference on Ant. and Propag. (EuCAP 2010), Barcelona, Spain, April 2010.

[12] R. A. Penchel, J. R. Bergmann, and F. Moreira, "Main-reflector shaping of omnidirectional dual reflectors using local conic sections," *IEEE Trans. Antennas Propag.*, vol. 61, pp. 4379–4383, Aug. 2013.

[13] J. R. Bergmann and F. J. S. Moreira, "Bandwidth behavior of omnidirectional dual-reflector antennas synthesized for uniform coverage," Journal of Microwaves, Optoelectronics, and Electromagnetic Applications, vol. 8, no. 1, pp. S1–S8, June 2009.

[14] F. Moreira and J. Bergmann, "Axis-Displaced Dual-Reflector Antennas for Omnidirectional Coverage with Arbitrary Main-Beam Direction in the Elevation Plane," *IEEE Trans. on Antennas and Propagation*, vol. 54, no. 10, pp. 2854–2861, Oct. 2006.

[15] F. Moreira and J. R. Bergmann, "Classical Axis-Displaced Dual-Reflector Antennas for Omnidirectional Coverage," *IEEE Trans. on Antennas and Propagation*, vol. 53, no. 9, pp. 2799—2808, Sept. 2005.

[16] S. Zang, J. Bergmann, Analysis of Omnidirectional Dual-Reflector Antenna and Feeding horn Using Moment Methods. *IEEE Transactions on Antennas and Propagation*. , v.62, no. 3, p.1534–1538, Mar. 2014.